Published in final edited form as:
Anal Chem. 1998 July 15; 70(14): 3033–3041.

Analysis of Isomeric Mixtures Using Blackbody Infrared Radiative Dissociation: Determining Isomeric Purity and Obtaining Individual Tandem Mass Spectra Simultaneously

Paul D. Schnier and **Evan R. Williams***
Department of Chemistry, University of California, Berkeley, California 94720

Abstract

A new method that makes possible, for the first time, simultaneous acquisition of individual dissociation mass spectra of isomeric ions in mixtures is presented. This method exploits the exquisite sensitivity of blackbody infrared radiative dissociation kinetics to minor differences in ion structure. Instead of separating precursor ions based on mass (isomers have identical mass), fragment ions are related to their original precursor ions on the basis of rate constants for dissociation. Mixtures of the peptide isomers des-R^1 and des-R^9 bradykinin are dissociated simultaneously at several temperatures. By fitting the kinetic data to double-exponential functions, the dissociation rate constant and abundance of each isomer in the mixture are obtained. To overcome the difficulty of fitting double-exponential functions, a novel global analysis method is used in which several dissociation data sets collected at different temperatures are simultaneously fit. The kinetic data measured at multiple temperatures are modeled with the preexponentials (corresponding to the abundance of each isomer) as “global” parameters which are constant for all data sets and the exponentials (rate constants) as “local” variables which differ for each data set. The use of global parameters significantly improves the accuracy with which abundances and dissociation rate constants of each individual compound can be obtained from the mixture data. Fragment ions produced from a mixture of these two isomers are related back to their respective precursor ions from the kinetic data. Thus, not only can the composition of the isomeric mixture be determined but an individual tandem mass spectrum of each component in the mixture can be obtained.

Tandem mass spectrometry (MS/MS) has many analytical advantages including high speed, sensitivity, and specificity and has been widely used for a variety of different applications in chemical analysis.[1–3] Complex mixtures can be rapidly screened for targeted compounds, even those present at trace levels.[1,2,4] In combination with soft ionization methods, such as matrix-assisted laser desorption/ionization[5] and electrospray ionization,[6] which can produce intact molecular ions of large molecules, MS/MS has been extended to the structural characterization of large molecules such as peptides and proteins[3,7,8] and oligonucleotides.[9–11] From structurally specific fragmentation, information about sequence,[12,13] locations of binding sites,[14–16] and posttranslational modifications[17–19] can be readily obtained.

For MS/MS of large ions, Fourier transform mass spectrometry (FTMS) has the advantage of multichannel detection over a wide mass range for high sensitivity, ultrahigh mass resolution and mass measuring accuracy, and compatibility with a variety of structural techniques.[12,20] Dissociation methods that have been applied to large ions include collisionally activated dissociation,[21,22] surface-induced dissociation,[23–25] and photodissociation using lasers[26,27] or blackbody radiation.[28–31] The later method, blackbody infrared radiative dissociation (BIRD), has the advantage that ions can be prepared with well-characterized internal energy distributions. From the temperature dependence of unimolecular dissociation rate constants, Arrhenius activation parameters for dissociation processes can be obtained. From these parameters, information about both the energetics and mechanisms of dissociation of large ions can be deduced.[29] Both the measured Arrhenius activation parameters and the dissociation

kinetics are exquisitely sensitive to small changes in ion structure and conformation. The Arrhenius parameters can differ significantly even for the formation of similar ions.[30]

An additional feature of FTMS is the ability to dissociate multiple precursor ions simultaneously. The resulting fragment ions can be related back to their respective precursor ions by uniquely encoding the fragmentation process for each precursor ion. Several methods to do this have been demonstrated.[32–35] One method encodes information in a second dimension using a sine function.[32,33] Many MS/MS spectra are acquired as the precursor excitation is modulated sinusoidally. The abundance of fragment ions formed by collisional activation or ion/molecule reactions of these precursors are modulated at the same frequency as the precursor ion. If each precursor ion is modulated at a different frequency, then a Fourier transform in this second dimension can be used to establish the relationship between the fragment ions and precursors. Precursor ion modulation can be effected by changing reaction times between two excitation wave forms[32] or by using tailored SWIFT wave forms.[33]

The fragment–precursor relationship can also be encoded digitally using zeros and ones.[34,35] This is the basis of the Hadamard transform method in which a Hadamard S-matrix encoding scheme is used to select half the precursors in a mixture and a combination MS/MS spectrum obtained.[34] For N precursors, N different combination spectra are acquired using a different combination of precursors for each. MS/MS spectra of the individual precursors are obtained from these combination spectra using a Hadamard transform. This method produces a signal-to-noise gain of $((N + 1)/2)^{1/2}$ or a time savings of $N/4$ over collecting the spectra individually.

These two-dimensional methods rely on the ability to differentiate precursor ions based on their mass. This is in general true of all MS/MS dissociation methods. If isomeric ions, which have identical mass, are present, a combination spectrum of the two isomer ions will be obtained. Here, we demonstrate a new method that makes possible the simultaneous acquisition of individual dissociation mass spectra of isomeric ions present in a mixture. With this method, the dissociation kinetics of isomeric mixtures are measured using BIRD. The fragment ions are related to the precursor ions by the rate constants for dissociation. Both individual mass spectra and the relative abundance of each precursor in the mixture are obtained. This method has the additional advantage over other two-dimensional methods in that all the precursor ions are dissociated simultaneously. Thus, no sample is wasted, although this method does require long data acquisition times.

EXPERIMENTAL SECTION

Materials.

Des-R^1 (PPGFSPFR) and des-R^9 (RPPGFSPF) bradykinin were purchased from Sigma Chemical Co. (St. Louis, MO) and were used without further purification. Standard stock solutions were made by dissolving 1.01 and 1.14 mg of des-R^1 and des-R^9 bradykinin, respectively, in 2.0 mL of water. The actual peptide content reported by Sigma is 73 and 81% by mass, respectively. The remaining mass consists of salts and water. The concentrations of these peptides in solution are calculated using these values. Aliquots (~50 μL) of these solutions were combined in various ratios and diluted by a factor of ~10 in 50/50 methanol/water to produce solutions with concentrations of $\sim 5 \times 10^{-5}$ M. Ions were formed by electrospray ionization using these diluted solutions.

Mass Spectrometry.

All BIRD experiments were performed on a 2.7-T FTMS instrument described in detail elsewhere.[28,29] Ions were formed with either nanoelectrospray[36] (flow rate ~60–200 nL/min) or standard electrospray (flow rate ~2 μL/min). Nanospray needles were made from 1.0-mm (o.d.) aluminosilicate capillaries pulled to a diameter of ~2-μm o.d. using a micropipet puller

(Sutter Instruments, Novato, CA.). A potential of ~900 V is applied to the solution using a Pt wire which is inserted into the back of the aluminosilicate capillary and held in place with a patch clamp holder (WPI Instruments, Sarasota, FL). Ions are guided from the electrospray ion source into a rectangular ion cell. Nitrogen gas is pulsed into the main chamber to facilitate ion trapping and thermalization. Isolation of the desired precursor was achieved using both single-frequency rf and SWIFT[37] excitation. The temperature of the vacuum chamber was controlled with a proportional temperature controller (Omega, Inc., Stamford, Ct.) and monitored with four copper–constantan thermocouples that surround the ion cell.

Mass spectra were acquired with an Odyssey data system (Finnigan-FTMS, Madison, WI). Ions were excited at a sweep rate of 1100 Hz/μs with direct-mode detection of 32–128K data points and an acquisition bandwidth of 940 kHz. For the kinetic data, the time-domain spectra were truncated to 32K data points, apodized with the Blackmann–Harris three-term function, and zero-filled once prior to performing a magnitude-mode Fourier transform.

Global Double-Exponential Curve Fitting.

Dissociation rate constants and abundances of individual components in a mixture of two isomers are determined by fitting the BIRD dissociation data to a double exponential of the form

$$y = Ae^{-at} + Be^{-bt} \tag{1}$$

where *A* and *B* are the gas-phase ion abundances and *a* and *b* are the dissociation rate constants of components A and B, respectively. Fitting data to a double-exponential function is, however, extremely unreliable since this is an ill-conditioned problem.[38,39] That is, several different combinations of fitting parameters (*A*, *a*, *B*, *b*) can be used to fit an individual data set.[38] To overcome this “multiple-minimum” problem, several BIRD dissociation data sets for the same mixture solution are collected at different temperatures. These data sets are then simultaneously fit to a double-exponential function (eq 1). This “global” fit is performed with the constraint, dictated by the experimental conditions, that the preexponentials (*A* and *B*) must be the same for each solution.

The method of indicator variables is used to perform global curve fits.[40,41] In this method, several data sets are simultaneously fit to double-exponential functions. Consider *N* experimental data sets each representing the dissociation spectra measured at a different temperature:

$$\left\{(t_1^1, y_1^1), (t_2^1, y_2^1), \ldots, (t_j^1, y_j^1)\right\}, \quad \text{data set 1}$$

$$\left\{(t_1^2, y_1^2), (t_2^2, y_2^2), \ldots, (t_k^2, y_k^2)\right\}, \quad \text{data set 2}$$

$$\left\{(t_1^N, y_1^N), (t_2^N, y_2^N), \ldots, (t_1^N, y_1^N)\right\}, \quad \text{data set } N$$

where each *y* is the normalized abundance of an ion at time *t*. These data sets are concatenated into a single data set, $S = \left\{(t_1^1, y_1^1) \ldots (t_k^N, y_k^N)\right\}$ which contains all data points measured at *N* temperatures. This data set is fit to the piece-wise defined function

$$y = x_1 Ae^{-a_1 t} + x_1 Be^{-b_1 t} + x_2 Ae^{-a_2 t} + x_2 Be^{-b_2 t} + \ldots + x_N Ae^{-a_N t} + x_N Be^{-b_N t} \tag{2}$$

where A and B are the preexponentials, a_i and b_i are the rate constants for dissociation of components A and B for data set i, and

$$x_i = \begin{cases} 1 \text{ if } (t,\ y) \in \text{data set } i \\ 0 \text{ otherwise} \end{cases}$$

for each data point. The x_i variables are called indicator or dummy variables.[40,41] Note that this function is equivalent to N independent double-exponential equations, with one equation representing each individual data set. S is fit to this equation using standard nonlinear χ^2 fitting.[42] The fitting parameters (A, B, a_1, b_1, ..., a_N, b_N) which minimize the error function χ^2

$$\chi^2 = \sum_1^M (y_i^j - y(t_i^j,\ A,\ B,\ a_1,\ b_1,\ \ldots,\ a_N,\ b_N))^2 \quad (3)$$

are determined, where the sum is taken over all data points in S and y is defined in eq 2. The standard Levenberg–Marquardt method for minimizing χ^2 is used.[42] Analysis is performed in the IGOR Pro (v. 3.01 for Macintosh, Wavemetrics Inc., Lake Oswego, OR) data analysis and programming environment using both built-in analysis functions and functions written in-house using the IGOR Pro programming language and C.

RESULTS AND DISCUSSION

Fragmentation Pathways and Kinetics.

Blackbody infrared radiative dissociation spectra of protonated des-R^1 and des-R^9 bradykinin measured individually at a temperature of 179 °C are shown in Figure 1. Different reaction times are required in order to produce similar extents of dissociation. This indicates that the rate constants for dissociation of these isomers differ at this temperature. The reaction times for the Figure 1a and b data are 30 and 120 s, respectively. Both ions dissociate by loss of water and cleavage at the second amide bond of the peptide backbone. For des-R^1 bradykinin, the charge is retained exclusively by the C-terminal fragment to form a y_6 ion (nomenclature of Roepstorf[43]). For des-R^9 bradykinin, both parts of the molecule compete for the proton resulting in complementary b_2/y_6 ions. Figure 1c shows a BIRD spectrum of a 56/44 des-R^9/des-R^1 bradykinin mixture measured at this same temperature (179 °C) with a 115-s reaction time. From this spectrum alone, it would be impossible to deduce the presence of the two isomers without a priori knowledge of the fragmentation of these precursors.

Dissociation rate constants are obtained from the BIRD data measured as a function of reaction time. Plots of $\ln\{[P^+]/([P^+] + \sum[F^+])\}$ of these data, where $[P^+]$ and $[F^+]$ are the abundances of the parent and fragment ions, respectively, are shown in Figure 2a for the pure components as well as three mixtures containing 44/56, 21/79, and 70/30 ratios of des-R^1 to des-R^9 bradykinin. These mixture solutions will subsequently be referred to as mixtures I–III, respectively. The natural log plots for pure des-R^1 and des-R^9 bradykinin are linear. From the slope of these data, dissociation rate constants (k) of 0.0106 and 0.0621 s^{-1} are obtained for des-R^1 and des-R^9 bradykinin, respectively.

In contrast, the natural log plots of data obtained from the mixtures are clearly nonlinear (Figure 2a). Nonlinear behavior can occur when the internal energy distribution of the ion population has not reached a steady state prior to the reaction time.[29] This problem can be eliminated by pulsing in a collision gas during the ion accumulation, as was done in this experiment. The nonlinearity observed here is due to the presence of two or more isomeric structures that have different dissociation rate constants. The nonlinearity becomes more difficult to discern as the relative amount of the fast-reacting component (des-R^9 bradykinin) in the mixture is decreased.

The time dependence of the total protonated precursor ion abundance ([P]; m/z = 905) of a mixture of these two isomers dissociated at a fixed temperature is given by eq 4, where $[P_1]_o$

$$[P] = [P_1]_o e^{-k_T^1 t} + [P_9]_o e^{-k_T^9 t} \quad (4)$$

and $[P_9]_o$ are the initial precursor ion abundances and k_T^1 and k_T^9 are the overall unimolecular dissociation rate constants for des-R^1 and des-R^9 bradykinin, respectively. Figure 2b shows the normalized abundance of [P] as a function of time for the dissociation of mixtures I–III at 179 °C. Also included are the theoretical curves calculated from eq 4 for these dissociation reactions using values of $[P_1]_o$ and $[P_9]_o$ from the known abundance of the species in solution and k_T^1 and k_T^9 from the dissociation constants of each isomer measured individually. The theoretical decay curves calculated using the known values for the individual components are in reasonable agreement with the experimental data points for the dissociation of the mixtures. This indicates that the abundance of the ions in the gas phase accurately represents the solution-phase abundances of these two isomers. Thus, there is not a significant difference in the ionization efficiency of these two peptides when electrosprayed from a mixture.

In principle, the individual rate constants and preexponentials (abundances) of each component in the mixture can be determined by fitting the normalized abundance of the precursor, [P], to a double-exponential function (eq 4). This has been done, for example, to determine relative percentages of conformational isomers from proton-transfer reaction kinetics.[44,45] However, fitting a sum of exponential equations is a difficult problem when the rate constants are similar. This is because many different combinations of parameters can often result in fits to the experimental data that are of similar quality.

Fitting double exponentials is a well-recognized problem in numerical analysis. “For it is well-known that an exponential equation of this type (eq 1) in which all four parameters are to be fitted is *extremely* ill conditioned. That is, there are many combinations of (*a*, *b*, *A*, *B*) that will fit most exact data quite well indeed (will you believe four significant figures?) and when experimental noise is thrown in the pot, the entire operation becomes hopeless.”[38] However, if one or more of the parameters can be fixed in multiple data sets where other parameters change, then the combination of parameters that will fit all the data can be drastically reduced. We subsequently refer to this as a global analysis. The problem of fitting double exponentials and the global fit solution is illustrated in the following section using simulated data. This method is applied to the actual experimental data in the subsequent section.

SIMULATED MIXTURE DISSOCIATION DATA

Fitting Double Exponentials.

In nonlinear least-squares curve fitting, a set of trial values for the fitting parameters is systematically varied.[42] The “best” values are ones that minimize χ^2. When fitting ill-conditioned functions, such as double exponentials in which the χ^2 error surface is relatively flat or possesses multiple minimums, the fit that is obtained can be highly dependent on the initial trial parameters.[39] This problem is illustrated using simulated data for a 60/40 mixture ($[P_1]_o$ = 0.60, $[P_2]_o$ = 0.40) with rate constants of 0.005 and 0.039 s^{-1} and 2% random noise added. Figure 3a shows three fits to this data set with different initial trial parameters which result in best-fit preexponential values of $[P_1]_o$ = 0.5, 0.62, and 0.72 and $[P_2]$ = 0.5, 0.38, and 0.28 with χ^2 values of 0.018, 0.024, and 0.027. These fits appear to reasonably model the data. However, the best fit (lowest χ^2) indicates a 50/50 mixture, a significant deviation from the

true value of 60/40. Furthermore, the answer obtained is highly dependent on the initial guess parameters. This is because the χ^2 surface is relatively flat.

To explore the entire χ^2 error surface for all possible fits, the data shown in Figure 3a is fit to eq 4 holding the preexponentials constant for each possible set of $[P_1]$ and $[P_2]$ such that $[P_1] + [P_2] = 1$. These values are varied systematically from 0.00 to 0.50 in increments of 0.02. That is, χ^2 is minimized for $[P_1] = 0.50$, $[P_2] = 0.50$; $[P_1] = 0.48$, $[P_2] = 0.52$; etc. Rate constants that represent the best fit to the data set for each set of preexponentials are found. The resulting minimized χ^2 values as a function of the preexponential are shown in Figure 4 (1 temperature, 41 data points). The minimum in χ^2 occurs at $[P_1] = [P_2] = 0.50$. Thus, the overall best fit to these simulated data incorrectly indicates a 50/50 mixture. However, the curve is relatively flat, which indicates that many different best-fit parameters exist for this data set that are nearly equally valid. This illustrates the well-known problem of fitting a single set of experimental data to a sum of exponentials.

Global Curve Fits.

More accurate information can be obtained from the double-exponential data if one or more parameters are fixed. This can be done in the BIRD experiments even if no a priori knowledge of the mixture is known. Dissociation rate constants vary as a function of temperature. The preexponential factors, which correspond to the abundance of the ions formed from solution, do not. Thus, if data from the same solution are obtained at more than one temperature, the preexponential factors in eq 4 remain constant for each data set. The data measured at two or more temperatures can be fit by treating the preexponentials as “global parameters” which are constant for all data sets. The rate constants are “local parameters” for which best fits are obtained for each individual data set. This data reduction method is often referred to as the method of fitting with indicator or dummy variables.[40,41]

This method is illustrated by use of simulated dissociation data of a 60/40 mixture using the Figure 3a data. A second data set is simulated using rate constants (k_1, k_2) 2.5 times larger than those in the Figure 3a data, again with 2% random noise added. Both simulated data sets are shown in Figure 3b. The two data sets are both fit individually and simultaneously treating the preexponentials as global variables and the rate constants as local variables for each data set. These data were fit by use of the same procedure outlined above using all possible combinations of preexponentials in increments of 0.02. As for the Figure 3a data set, the values of χ^2 for the faster data set fit individually do not change significantly with the mole fraction. The minimum on the χ^2 surface is located at 0.66/0.34. Thus, the best fit to these data incorrectly indicates a 66/34 mixture. Use of the global fitting procedure on both data sets results in a minimum in the χ^2 surface which is deeper and more clearly defined (Figure 4; 2 temperatures, 80 points). In addition, the minimum is located at 0.60/0.40, which correctly indicates a 60/40 mixture.

An increase in the number of data sets at different temperatures results in a further improvement in the quality of the global fit. This is illustrated in Figure 3c and d using data calculated at three and six different temperatures, respectively. Also included in this figure are the global fits to these data The corresponding χ^2 values for all possible mole fractions are shown in Figure 4. As the number of data sets at different temperatures increases, it is clear that the best fit (minimum χ^2) is much more clearly defined. Thus, this global analysis method can greatly reduce the number of solutions that satisfy eq 4 and can dramatically reduces the multiple-minimum problem for ill-conditioned functions.

Effect of Number of Data Points.

In this previous analysis, an increase in the number of data sets at different temperatures also increases the number of data points in the fitting procedure. An increase in the number of data

points even at one temperature will result in an improved fit. However, for an analysis with a fixed number of data points, acquiring data sets at several different temperatures with subsequent global analysis can provide better information than measuring a single data set at one temperature with an equal number of total data points.

This is illustrated by fitting one simulated data set containing 240 data points for a 60/40 mixture, using the same rate constants as the data set in Figure 3a and 2% noise. The χ^2 values for these data as a function of mole fraction are given in Figure 4. The χ^2 curve for this larger data set is much steeper and the minimum is more clearly defined than the single data set with 41 points. In addition, the minimum is located at approximately the correct value (60/40) vs 50/50 for the data set containing fewer data points.

The χ^2 curve (Figure 4) for the global fit to 6 data sets, which also include a total of 240 data points, is also given (Figure 3d data). For preexponential values far from the correct values, the two curves have similar slopes. However, the curve for the one large data set is much flatter near the minimum. The curve for the six data sets has a minimum on the χ^2 surface at 60/40 which is much more clearly defined. This demonstrates that the benefit of the global analysis method is not simply due to a larger number of data points, but rather a decrease in the ratio of fitting parameters to equations. This greatly reduces the number of combinations of parameters that satisfy eq 4. Thus, for a fixed number of data points, e.g., if the analysis is time- or sample-limited, collecting smaller data sets at two or more different temperatures is better than collecting one large data set. The relative merit of these two approaches depends on the total number of data points acquired.

EXPERIMENTAL MIXTURE DISSOCIATION DATA

Relative Abundance.

The experimental BIRD data for mixtures I–III were fit using the global fitting procedure described and demonstrated previously using the simulated data. The experimental data and the global fits to these data are shown in Figure 5. For mixture I, the preexponentials obtained from the global fit are 0.53 and 0.44 for the fast- and slow-reacting species, respectively (Table 1). This is in excellent agreement with the ratio of these isomers in solution (0.56/0.44). In order for there to be quantitative agreement between the preexponentials obtained by this method and the solution data, the ionization efficiencies of the two components and the detection efficiencies of the product ions must be the same. These results indicate that both these factors must be comparable for these two similar peptide ions. The rate constants for the two components obtained from the global fit are also very close to the rate constants for each component measured individually. Thus, it is possible not only to readily identify the existence of multiple dissociating populations but also to quantitate the abundance of each of these species and accurately measure the rate constants for dissociation at multiple temperatures.

The results for the other mixtures are also given in Table 1. The agreement for mixture II is also very good for both the preexponentials and the rate constants. The agreement between the prexponentials for mixture III and the actual solution values is worse. As the ratio of slow-reacting species is increased, the accuracy of the data needed to extract the individual kinetic parameters and abundances of the two dissociating species increases significantly. This is illustrated qualitatively in Figure 2a, which shows plots of $\ln\{[P^+]/([P^+] + \sum[F^+])\}$ vs time for these three mixtures. As the relative abundance of des-R^1 bradykinin (the slow component) in the mixture is increased, the nonlinear behavior becomes more difficult to discern.

General Procedure for Extracting Individual Tandem Mass Spectra.

If two isomeric ions dissociate with different rate constants, then the fragment ions produced from a mixture of these two isomers can be related back to their respective precursor ions on the basis of these rate constants. This is illustrated in Figure 6, which shows an appearance/depletion curve for dissociation of *m*/*z* 905 ions from mixture I measured at 160 °C. The abundances of the fragment ions at *m*/*z* 254 and 651 increase rapidly for ~100 s but then level off at longer time. In contrast, the abundance of the ion at *m*/*z* 711 is still increasing at 700 s. The kinetics for formation of these ions fit a single exponential indicating that these ions are formed from only one precursor. The more rapid appearance of the *m*/*z* 254 and 651 ions indicates that they are formed from the precursor that has the faster dissociation rate constant (des-R^9 bradykinin). The slower appearance of the *m*/*z* 711 ion indicates that it is formed from the slower dissociating precursor (des-R^1 bradykinin). The abundance of the ion at *m*/*z* 887 increases very rapidly at the start but then increases more slowly even at times up to 700 s. These data do not fit a single exponential but do fit a double exponential indicating that this ion is formed from both precursor ions.

These data can be quantitatively fit using the following procedure. A general dissociation scheme for dissociation of two parent ions by parallel reactions to yield the product ions, F_1–F_n, is given by

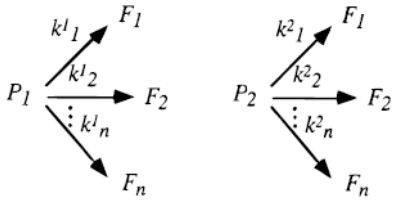

where k_i^1 and k_i^2 are the rate constants for formation of each fragment F_i, from P_1 and P_2, respectively. This reaction scheme is valid for any number of parallel reactions from two precursors but does not include subsequent dissociation of fragment ions. If a fragment ion, F_i, is formed from only one parent ion, then k_n from the other parent is 0. The overall unimolecular dissociation rate constants for the depletion of P_1 and P_2, k_T^1 and k_T^9, respectively, are given by

$$k_T^1 = k_1^1 + k_2^1 + \ldots + k_n^1 \quad k_T^2 = k_1^2 + k_2^2 + \ldots + k_n^2 \tag{5}$$

For this dissociation scheme, the integrated rate law for the appearance of each fragment ion, F_i, as a function of time is given by eq 6, where k_T^1 and k_T^2 are the overall dissociation rate

$$[F_i] = \frac{k_i^1[P_1]_o}{k_T^1}(1 - e^{-k_T^1 t}) + \frac{k_i^2[P_9]_o}{k_T^2}(1 - e^{-k_T^2 t}) \tag{6}$$

constants for each parent ion. These values, as well as $[P_1]_o$ and $[P_2]_o$, are determined from the depletion of the precursor ion using the global fitting procedure outlined above.

The fragment–precursor relationship can be determined by fitting the fragment ion abundances to a double-exponential function. That is, the precursor of each fragment ion is “encoded” by the rate constant for the fragment ion formation. The contribution of each precursor to the fragment ion abundance is determined from the relative values of the preexponentials. If, for example, the preexponential for k_T^1 is zero, this indicates that this fragment ion does not come

from precursor one. Since the values of k_T^1 and k_T^2 are determined from the global fitting procedures, these values are fixed in fitting the fragment ion data. This eliminates the multiple-minimum problem in fitting these data to a double-exponential function. If the value of one preexponential is significantly smaller than the other or is a negative value, then the data are fit to a single exponential to obtain more accurate values for k_i^1 or k_i^2. Dissociation spectra of each individual precursor ion at any extent of dissociation can be calculated from these rate constants.

Determining Individual Mass Spectra.

The procedure to obtain individual mass spectra is illustrated using the Figure 6 data. The overall rate constants, k_T^1 and k_T^2, and initial abundances, $[P_1]_o$ and $[P_2]_o$, are obtained from the global fitting procedure at multiple temperatures. To determine the origin of each fragment ion, the normalized abundance of each fragment ion, $(1 - [F_i])$, is fit to a double-exponential function. The exponential terms k_T^1 and k_T^2 in eq 6 are fixed, eliminating the multiple-minimum problem of double-exponential fitting. These fits to the fragment ion data from mixture I are included in Figure 6. The preexponentials obtained are given in Table 2. If one of the preexponentials is small (or negative), it indicates that the fragment is not generated from the parent with the overall rate constant given by that exponent. This is the case for the ions at *m*/*z* 711, 651, and 254. Fragment ions at *m*/*z* 254 and 651 are formed from the fast-reacting component (des-R^9 bradykinin), the fragment at *m*/*z* 711 is formed from the slow-reacting component (des-R^1 bradykinin), and the fragment at *m*/*z* 887 comes from both parents. These results are consistent with the known fragmentation of these two ions. From these preexponentials (Table 2), the rate constants for the formation of each product ion are readily calculated from eq 6. For the fragment ions formed from only one precursor, more accurate rate constants for formation can be obtained by fitting the data to a single exponential.

The fragment ion abundance resulting from the dissociation of each precursor ion can be calculated at any dissociation time from the integrated rate laws given by eqs 4 and 6. Thus, individual tandem mass spectra of both precursor ions can be determined from a mixture. This is illustrated using the data for mixture I dissociated at 160 °C. The BIRD spectra of des-R^9 and des-R^1 bradykinin measured individually with reaction times of 90 and 180 s, respectively, are shown in Figure 7. The calculated spectra of these two isomers obtained from the mixture data are indicated by an “X” on the figure. The extracted mass spectra from the simultaneous dissociation of these isomers are in excellent agreement with the tandem mass spectra measured individually.

Sample Consumption.

Acquisition of the BIRD kinetic data can take many hours due to the long reaction times used (up to 700 s in this work). For example, the data in Figure 6 required ~3 h to acquire during which time sample was continuously electrosprayed. With nanospray, which was used to obtain these data, only ~3 μL of sample was consumed. This corresponds to ~150 pmol of total material. The actual amount of sample required for this analysis is considerably less. Ions are injected into the FTMS cell typically for 3 s prior to the reaction time. Thus, the amount of time that ion formation is required is only a small fraction of the total analysis time. If voltage were applied to the solution only during the time necessary for ion production and not during the BIRD reaction time, the amount of material consumed could be reduced by a factor of ~50. Thus, this method could be applied to mixtures where significantly less sample is available.

Effect of Ion Accumulation Time.

The temperature of the main vacuum chamber is maintained at a constant elevated temperature for the entire time during which a data set is acquired. During the ion accumulation time, ion dissociation can occur prior to the isolation of the precursor ions. If the ion accumulation time is significant compared to the overall reaction time, then the relative abundance of two isomers that have different dissociation kinetics will differ from the original ion composition formed by ESI. This effect is illustrated in Figure 2b (inset), which shows two dissociation data sets for mixture I measured at 179 °C using ion accumulation times of 3 and 7 s, but otherwise measured under identical conditions. The 4-s increase in ion accumulation time has a measurable effect on the dissociation curve despite the fact that the dissociation experiment is carried out to 200 s. The des-R^9 bradykinin, which has a faster dissociation rate constant at this temperature, is preferentially depleted before the ion isolation. This leads to an enrichment of the slower reacting des-R^1 bradykinin in the starting precursor ion mixture and slower dissociation kinetics. The dissociation curve of this mixture is shifted to longer times.

The load time in these experiments was typically 3 s so that any ion dissociation that occurs during this time should have only a minimal effect on the abundance results. This is consistent with our results that indicate the ion abundance obtained from our ion mixture analysis accurately reflect the solution-phase composition. The effect of ion accumulation time could reduce the accuracy of mixture analyses in cases where signal is difficult to generate and significantly longer ion accumulation times are required.

Arrhenius Parameters.

An important advantage of the BIRD experiments is the ability to obtain Arrhenius activation parameters for the dissociation of larger ions from the temperature dependence of the dissociation rate constants. These parameters provide information about both the dissociation energetics and mechanisms. Individual Arrhenius parameters for des-R^1 and des-R^9 bradykinin can be obtained from the mixture data using the extracted individual dissociation rate constants at the three temperatures. For example, the activation energies obtained from the mixture II data are 1.1 ± 0.2 and 1.0 ± 0.2 eV and log *A* values are 10 ± 2 and 9 ± 2 for these ions, respectively. The large error in these values is primarily due to the limited number of data sets (three temperatures). Within these uncertainties, the Arrhenius parameters are in agreement with the more accurate values measured previously for the individual ions.[30]

CONCLUSIONS

Isomeric mixtures are difficult to analyze by conventional tandem mass spectrometry methods in which an ion is mass selected and dissociated. Because isomeric ions have the same mass, dissociation of multiple isomers results in a combination tandem mass spectrum from which the individual contributions of the different isomers is difficult or impossible to obtain without a priori knowledge. The method presented here makes possible simultaneous acquisition of individual dissociation mass spectra of isomers present in mixtures. Mixtures consisting of different amounts of two peptide isomers are dissociated using BIRD at multiple temperatures. From the dissociation data, the abundances of the two ions are obtained using a global analysis data reduction method. This method overcomes the problems of fitting double-exponential functions to a single data set and makes possible more accurate results. The fragment ions are related back to the precursor ions from which they are formed by the rate constants for precursor ion dissociation. From appearance/depletion curves, rate constants for fragment ion formation are determined. With these values, the individual dissociation spectrum of each component can be obtained at any extent of dissociation.

This method is analogous to other two-dimensional multiplexing methods implemented in FTMS, such as the Hadamard transform and Fourier transform methods. This method has the additional advantages that it can be applied directly to isomeric mixtures and that all ions are dissociated simultaneously so that no sample is wasted. While demonstrated here for a mixture containing two isomers, this method could in principle be extended to significantly more complicated mixtures. To obtain accurate abundances from multicomponent isomeric mixtures, the ions must have significantly different rate constants for dissociation. Because BIRD kinetics are exquisitely sensitive to small differences in ion structure, this method could be useful for analyzing the isomeric purity of large proteins and DNA as well as quantitating and identifying isomers present in synthetic libraries.

Acknowledgements

This research has been made possible by generous financial support from the National Science Foundation (Grant CHE-9726183), National Institutes of Health (Grant 1R29GM50336-01A2), and the Society of Analytical Chemists of Pittsburgh for sponsoring fellowship support though the American Chemical Society, Division of Analytical Chemistry (P.D.S.).

References

1. McLafferty, F. W. Tandem Mass Spectrometry; John Wiley and Sons: New York, 1983.
2. Busch, K. L.; Glish, G. L.; McLuckey, S. A. Mass Spectrometry/Mass Spectrometry: Techniques and Applications of Tandem Mass Spectrometry; VCH Publishers: New York, 1988.
3. McLafferty FW. Acc Chem Res 1994;27:379–386.
4. Hoke SH, Wood JM, Cooks RG, Li XH, Chang CJ. Anal Chem 1992;64:2313–2315. [PubMed: 1361307]
5. Hillenkamp F, Karas M, Beavis RC, Chait BT. Anal Chem 1991;63:1193A–1202A. [PubMed: 1897719]
6. Fenn JB, Mann M, Meng CK, Wong SF, Whitehouse CM. Science 1989;246:64–71. [PubMed: 2675315]
7. Valaskovic GA, Kelleher NL, McLafferty FW. Science 1996;273:1199–1202. [PubMed: 8703047]
8. Dongre AR, Somogyi A, Wysocki VH. J Mass Spectrom 1996;31:339–350. [PubMed: 8799282]
9. McLuckey SA, Habibigoudarzi S. J Am Chem Soc 1993;115:12085–12095.
10. McLafferty FW, Aaserud DJ, Guan ZQ, Little DP, Kelleher NL. Int J Mass Spectrom Ion Processes 1997;165:457–466.
11. Pomeramtz NJ, Rozenski J, Zhang Y, McCloskey JA. Anal Chem 1996;68:1989–1999. [PubMed: 9027217]
12. Bowers MT, Marshall AG, McLafferty FW. J Phys Chem 1996;100:12897–12910.
13. O'Connor PB, Speir JP, Senko MW, Little DP, McLafferty FW. J Mass Spectrom 1995;30:88–93.
14. Costello CA, Kelleher NL, Abe M, McLafferty FW, Begley TP. J Biol Chem 1996;271:3445–3452. [PubMed: 8631946]
15. Kelleher NL, Costello CA, Begley TP, McLafferty FW. J Am Soc Mass Spectrom 1995;6:981–984.
16. Zaia J, Jiang L, Han MS, Tabb JR, Wu Z, Fabris D, Fenselau C. Biochemistry 1996;35:2830–2835. [PubMed: 8608118]
17. Michel H, Griffin PR, Shabanowitz J, Hunt DF, Bennett J. J Biol Chem 1991;266:17584–17591. [PubMed: 1894641]
18. Huddleston MJ, Bean MF, Carr SA. Anal Chem 1993;65:877–884. [PubMed: 8470819]
19. Kelleher NL, Nicewonger RB, Begley TP, McLafferty FW. J Biol Chem 1997;51:32215–32220. [PubMed: 9405424]
20. Buchanan MV, Hettich RL. Anal Chem 1993;65:245A–259A.
21. Senko MW, Speir JP, McLafferty FW. Anal Chem 1994;66:2801–2808. [PubMed: 7978294]
22. Wu Q, Van Orden S, Cheng X, Bakhtiar R, Smith RD. Anal Chem 1995;67:2498–2509. [PubMed: 8686880]

23. Williams ER, Henry KD, McLafferty FW, Shabanowitz J, Hunt DF. J Am Soc Mass Spectrom 1990;1:413–416.
24. Ijames CF, Wilkins CL. Anal Chem 1990;62:1295–1299. [PubMed: 2372128]
25. Chorush RA, Little DP, Beu SC, Wood TD, McLafferty FW. Anal Chem 1995;67:1042–4046. [PubMed: 7536399]
26. Little DP, Speir JP, Senko MW, O'Connor PB, McLafferty FW. Anal Chem 1994;66:2809–2815. [PubMed: 7526742]
27. Guan ZQ, Kelleher NL, O'Connor PB, Aaserud DJ, McLafferty FW. Int J Mass Spectrom Ion Processes 1996;158:357–364.
28. Price WD, Schnier PD, Williams ER. Anal Chem 1996;68:859–866.
29. Schnier PD, Price WD, Strittmatter EF, Williams ER. J Am Soc Mass Spectrom 1997;8:771–780. [PubMed: 16554908]
30. Schnier PD, Price WD, Jockusch RA, Williams ER. J Am Chem Soc 1996;118:7178–7189. [PubMed: 16525512]
31. Gross DS, Zhao Y, Williams ER. J Am Soc Mass Spectrom 1997;8:519–524. [PubMed: 16479269]
32. Pfandler P, Bodenhausen G, Rapin J, Walser ME, Gäumann T. J Am Chem Soc 1988;110:5625–5628.
33. Ross CW III, Guan S, Grosshans PB, Ricca TL, Marshall AG. J Am Chem Soc 1993;115:7854–7861.
34. Williams ER, Loh SY, McLafferty FW, Cody RB. Anal Chem 1990;62:698–703. [PubMed: 2327586]
35. Haebel S, Gäumann T. Int J Mass Spectrom Ion Processes 1995;144:139–166.
36. Wilm M, Mann M. Anal Chem 1996;68:1–8. [PubMed: 8779426]
37. Marshall AG, Wang TC, Ricca TL. J Am Chem Soc 1985;107:7893–7897.
38. Acton, F. S. Numerical Methods That Work; Harper & Row Publishers: New York, 1970.
39. Sivia, D. S. Data Analysis: A Bayesian Tutorial; Oxford University Press: Oxford, 1997.
40. Montgomery, D. C.; Peck, E. A. Introduction to Linear Regression Analysis; John Wiley & Sons: New York, 1982.
41. Cuthbert, D.; Wood, F. S. Fitting Equations to Data: Computer Analysis of Multifactor Data, 2nd ed.; Wiley & Sons: New York, 1980.
42. Press: W. H.; Flannery, B. P.; Teukolsky, S. A.; Vetterling, W. T. Numerical Recipes in Pascal; Cambridge University Press: Cambridge, 1989.
43. Roepstorff P, Fohlman J. J Biomed Environ Mass Spectrom 1984;11:601.
44. Gross DS, Schnier PD, Rodriguez-Cruz SE, Fagerquist CK, Williams ER. Proc Natl Acad Sci USA 1996;93:3143–3148. [PubMed: 8610183]
45. Cassady CJ, Carr SR. J Mass Spectrom 1996;31:247–254. [PubMed: 8799276]

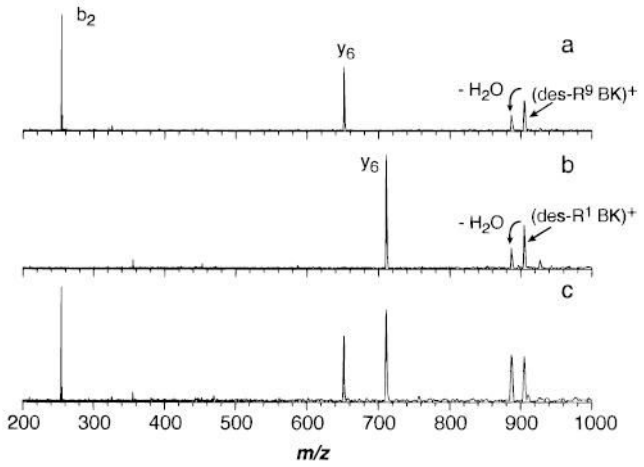

Figure 1.

Blackbody infrared radiative dissociation spectra of singly protonated (a) des-R^9 bradykinin (30-s reaction time), (b) des-R^1 bradykinin (120-s reaction time), and (c) 44%/56% des-R^1/ des-R^9 bradykinin mixture (mixture I, 115-s reaction time), measured at 179 °C.

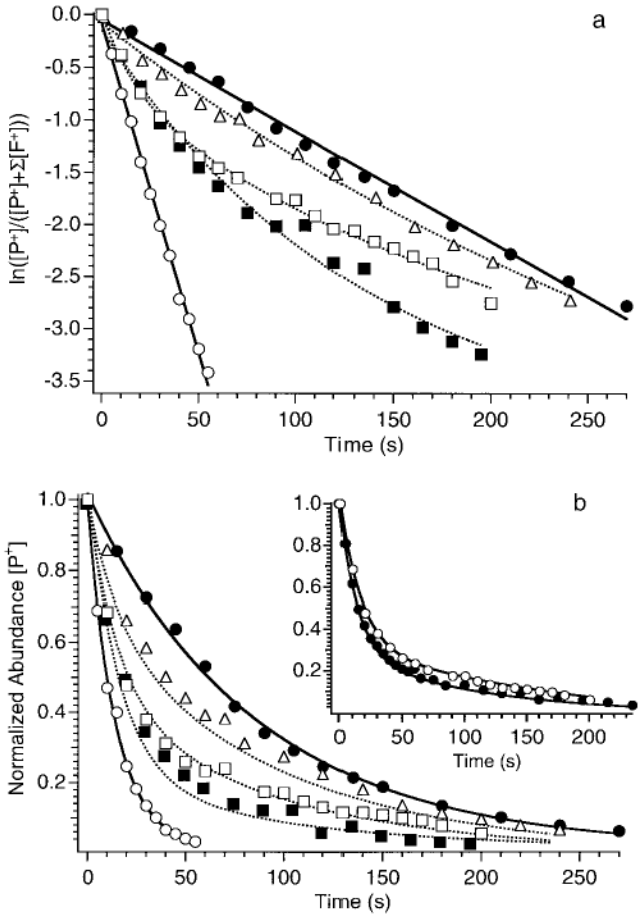

Figure 2.
Blackbody infrared radiative dissociation data of des-R^9 bradykinin (○), des-R^1 bradykinin (•), mixture I (□), mixture II (▪), and mixture III (▵) measured at 179 °C shown as (a) a natural log plot and (b) a normalized precursor ion abundance plot. Dotted lines in (b) are calculated depletion curves for each mixture using the rate constants measured for each individual isomer and solution abundances of the isomers. Inset shows depletion of precursor ions for mixture I using an ion accumulation time of 3 (•) and 7 s (○).

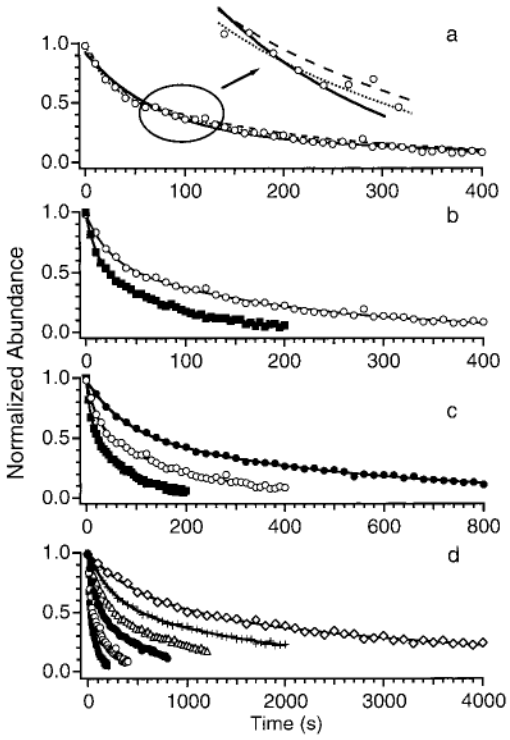

Figure 3.

(a) Three double-exponential fits to simulated 60/40 mixture dissociation data with rate constants of 0.005 and 0.039 s^{-1}, with 2% random noise added. The dotted, dashed, and solid lines have preexponentials of $[P_1]_o$ = 0.5, 0.62, and 0.72 and $[P_2]$ = 0.5, 0.38, and 0.28, respectively. (b–d) Global fits to simulated 60/40 mixture data, calculated using rate constants (s^{-1}) of (b) (0.005, 0.039), (0.0141, 0.0019); (c) (0.0125, 0.0975), (0.005, 0.039), (0.0141, 0.0019); and (d) (0.0125, 0.0975), (0.005, 0.039), (0.0141, 0.0019), (0.0069, 0.000 95), (0.0042, 0.000 49), and (0.001 86, 0.000 24).

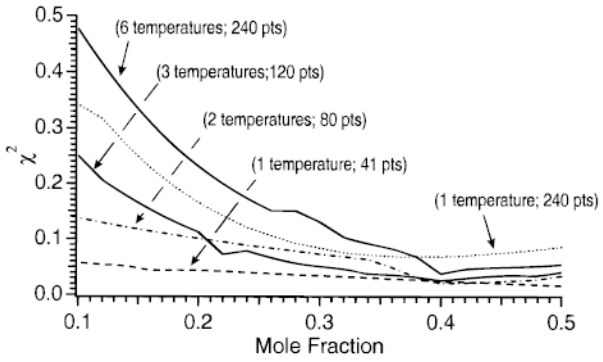

Figure 4.

χ^2 values for the best-fit parameters of simulated 60/40 mixture data as a function of preexponential values. The number of data sets corresponding to different temperatures and total number of data points is indicated.

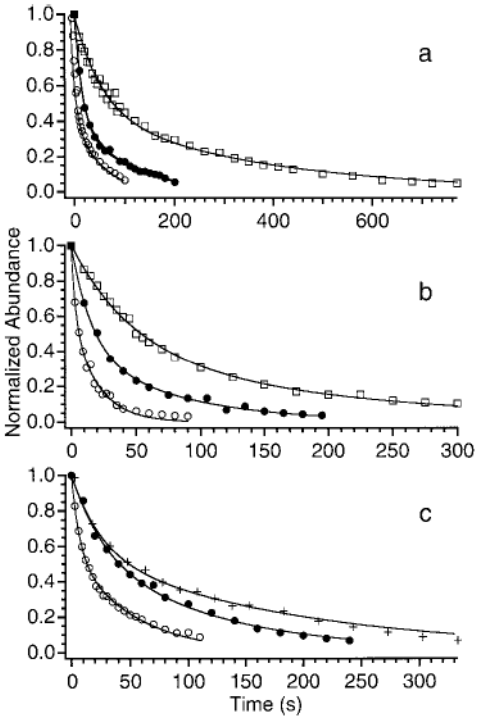

Figure 5.

Experimental BIRD data and global fits to the depletion of precursor ions for three des-R^1/des-R^9 bradykinin mixture: (a) I, (b) II, and (c) III. Dissociation data were measured at (□) 160, (+) 171, (•) 179, and (○) 191 °C.

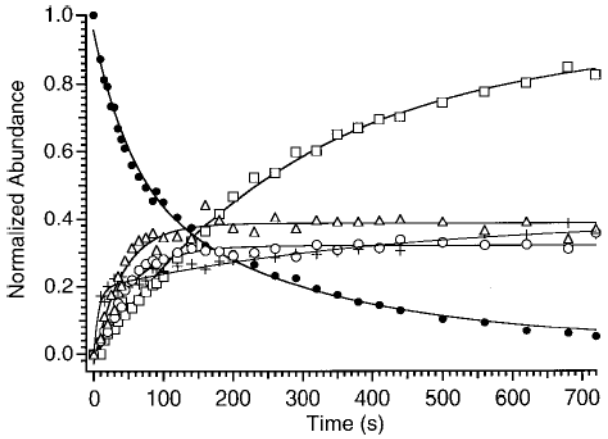

Figure 6.

Appearance/depletion data for mixture I at 160 °C fit to double-exponential functions: (•) *m*/*z* = 905; (+) *m*/*z* = 887; (□) *m*/*z* = 711; (○) *m*/*z* = 652; and (Δ) *m*/*z* = 254. Fragment ion abundances are multiplied by 2.

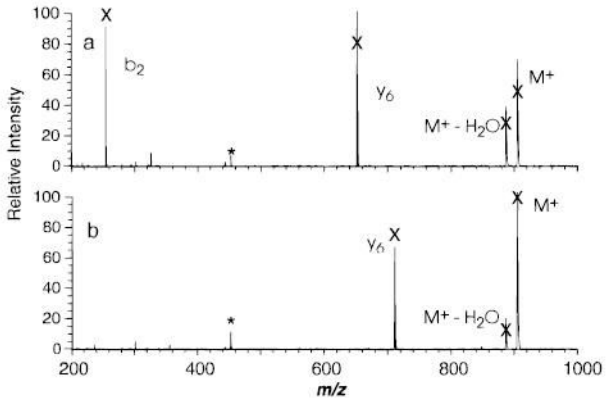

Figure 7.

Blackbody infrared radiative dissociation spectra of (a) des-R^9 bradykinin (90-s reaction time) and (b) des-R^1 bradykinin (180-s reaction time) measured at 160 °C. Xs indicate the calculated ion abundance for the individual ions obtained from mixture I measured at 160 °C. * denotes harmonics.

Table 1

Abundances and Rate Constants of des-R^1 and des-R^9 Bradykinin Measured Individually and from Global Double-Exponential Fits to Kinetic Data from Three Mixtures

des-R^1/des-R^9 bradykinin	temp (°C)	des-R^1/R^9 BK from double-exp fit	k_T from double-exp fit (s^{-1})		k_T measd individually (s^{-1})	
			des-R^1 BK	des-R^9 BK	des-R^1 BK	des-R^9 BK
mixture I						
44%/56%	160	46.0%/53.1%	0.003	0.018	0.003	0.015
	179		0.010	0.078	0.011	0.063
	191		0.016	0.121	0.019	0.113
mixture II						
21%/79%	160	29.5%/71.1%	0.004	0.019	0.003	0.015
	179		0.010	0.052	0.011	0.063
	191		0.025	0.121	0.019	0.113
mixture III						
70%/30%	171	56.2%/44.7%	0.004	0.051		
	179		0.008	0.035	0.011	0.063
	191		0.019	0.144	0.019	0.113

Table 2

Preexponentials from the Fragment Ion Kinetic Data for Mixture I at 160 °C

ion *m*/*z*	preexponential	
	k_1 (0.003 s^{-1})	k_9 (0.020 s^{-1})
254	−0.03	0.23
651	−0.002	0.16
711	0.47	−0.009
887	0.062	0.063